Electronic Supporting Information

Probing nonlinear optical coefficients in self-assembled peptide nanotubes

Soma Khanra[1], Kartik Ghosh[2], Fabio F. Ferreira[3], Wendel A. Alves[3], Francesco Punzo[4], Ping Yu[1], and Suchismita Guha[11]

[1]Department of Physics and Astronomy, University of Missouri, Columbia, MO 65211, USA

[2]Physics, Astronomy, and Materials Science, Missouri State University, Springfield, MO 65897, USA

[3]Centro de Ciências Naturais e Humanas, Universidade Federal do ABC, 09219-580 Santo Andre, Sao Paulo, Brazil

[4]Dipartimento di Scienze del Farmaco, Sezione Chimica, Università degli Studi di Catania, Viale Andrea Doria 6, 95125 Catania, Italy

[1] E-mail address: guhas@missouri.edu

I. SHG data at incident angles of 45° and 0° degree.

The tubes were oriented parallel to the plane of incidence.

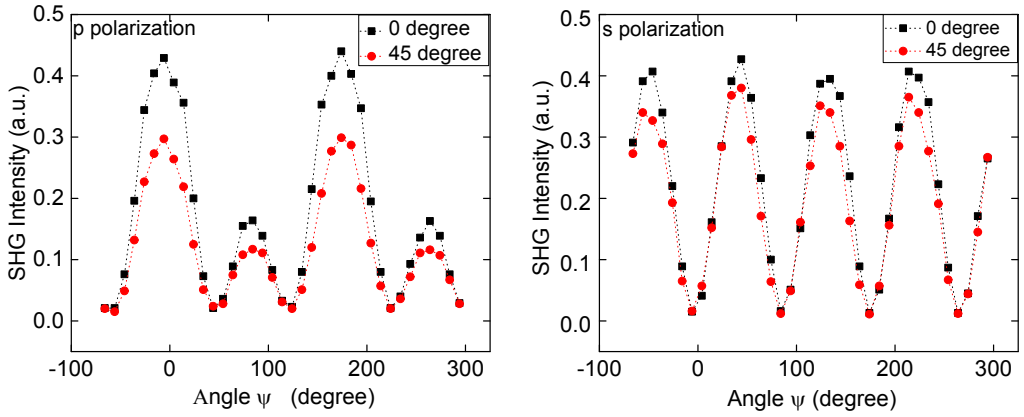

Figure S1 (a): *p*- and *s*- polarization data from a FF-MNT at 45° and 0° degree. There is a slight change in the SHG intensity due to the Fresnel coefficients of fundamental and SHG waves.

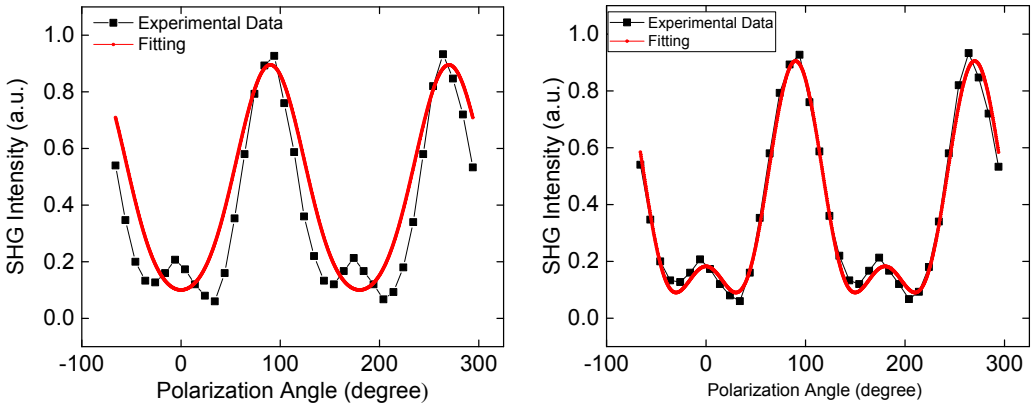

Figure S1 (b): *p*-polarization data at 0° degree fit with d_{31} and d_{33} having the same sign (left) and opposite sign (right).

II. SHG polarimetry from different orientations of FF-MNTs. *s* polarization data was fitted with Eq. (3a) to determine the orientation angle of the tubes. A small DC background had to be applied. The modified eq. used for the fits is: $P_{x'} = (A\sin 2(\Psi + \varphi))^2 + C$, where A and C are fitting parameters.

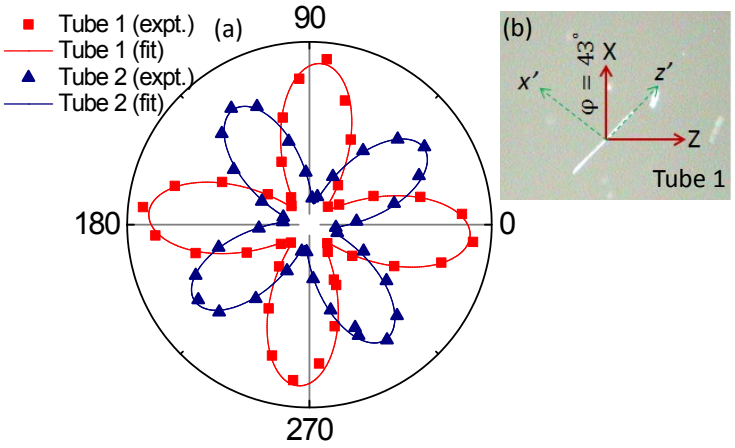

Figure S2. (a) Symbols are the experimental *s* polarization SHG data for two tube orientation. The solid lines are a fit to the square of Eq. (3 a). (b) Optical image of FF-MNT (Tube 1) (in white) where the angle was measured as 43° with respect to the laboratory frame of reference. For tube 2, the measured angle was 169°.

Table S1. SHG intensity was measured from individual FF-MNTs oriented at different angles. The second column shows the measured angle from the optical image and the third column shows the calculated angle from eq 3(a), confirming the $P6_1$ symmetry of the tubes.

Sample	Measured angle φ (°) from optical image	Calculate angle φ (°) from fit
FF-MNT 1	43±1	41.0±0.2
FF-MNT 2	169±1	168.0±0.5
FF-MNT 3	133±1	136.0±0.7
FF-MNT 4	77±1	76.0±0.5
FF-MNT 5	35±1	32.0±0.4
FF-MNT 6	82±1	82.0±0.2

III. SEM and SHG polarimetry of two FF-MNTs with approximately similar lengths but different diameters, where the SHG polarization pattern changes with the diameter.

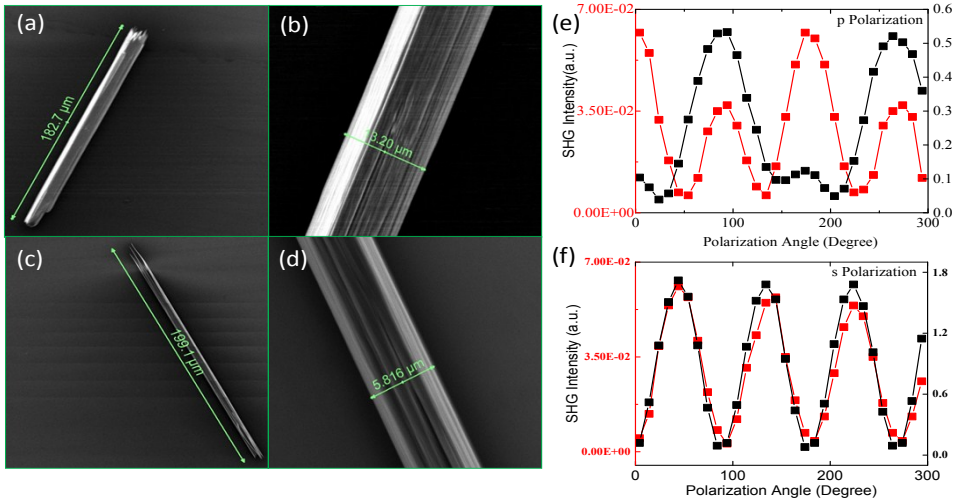

Figure S3: (a) and (b) are the SEM images from a FF-MNT with O.D. =13.2 µm. (c) and (d) are SEM images from a FF-MNT with O.D.=5.8 µm. (e) and (f) p-polarization and s-polarization SHG from the two tubes. The red curve represents the FF-NT with O.D. = 5.8 µm and the black curve represents the FF-MNT with O.D. =13.2 µm

IV. Absorption spectrum

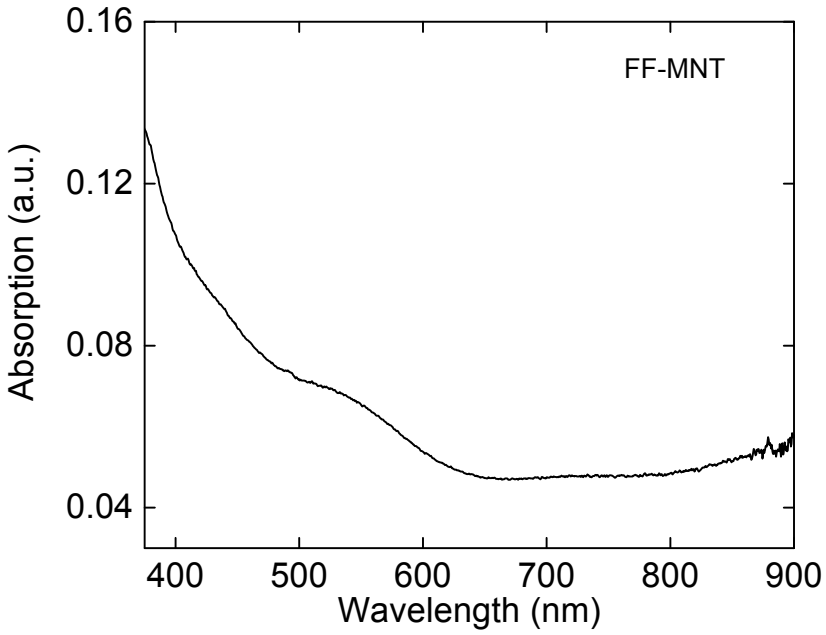

Figure S4. Absorption spectrum of FF-MNT.

V. XRD measurements from FF-MNT powder with different annealing conditions and Rietveld refinement

Table S2. Profile-weighed parameters (R_{wp}) extracted from Rietveld refinement. The first column lists the annealing temperatures. a, b, c and V are the unit cell parameters. B_{iso} and B_{iso_H} are the isotropic displacement parameters of non-hydrogen and hydrogen atoms, respectively. The last column shows the calculated density from the X-ray data.

sample ID	R_{wp} (%)	a (Å)	c (Å)	Vol (Å^3)	B_{iso}	B_{iso_H}	Density (g cm^{-3})
RT	2.502	24.104(2)	5.4460(5)	2740.1(5)	3.5(6)	4.2(7)	1.212(4)
80 °C	2.477	24.106(1)	5.4419(4)	2738.7(4)	3.7(4)	4.5(5)	1.208(3)
135 °C	2.606	24.118(1)	5.4424(3)	2741.7(3)	4.6(3)	5.5(4)	1.208(2)
sample ID	R_{wp} (%)	a (Å)	b (Å)	c (Å)	Vol (Å^3)	B_{iso}/B_{iso_H}	Density (g cm^{-3})
150 °C	2.369	6.164(3)	10.315(6)	23.840(11)	1515.7(14)	5.1(11)/6.1(13)	1.290(1)

Table S3. Morphology Predictions for IFABEW, CCDC #1494530 and DUZDUX. % of Total Facet Area (Å^2) is Calculated as 100 × (hkl facet area)/(total surface area)

IFABEW (Hex-I)					
hkl	Multiplicity	Area	% Area	Total area	% Total area
{0 1 0}	6	$4.01 \cdot 10^4$	16.083	$2.406 \cdot 10^5$	96.50
{1 -1 1}	6	727.11	0.292	$4.363 \cdot 10^3$	1.75
{1 -1 -1}	6	727.11	0.292	$4.363 \cdot 10^3$	1.75
CCDC #1494530 (Hex-II)					
hkl	Multiplicity	Area	% Area	Total area	% Total area
{0 1 0}	6	$3.64 \cdot 10^4$	16.120	$2.182 \cdot 10^5$	96.72
{1 -1 1}	6	616.34	0.273	$3.698 \cdot 10^3$	1.64
{1 -1 -1}	6	616.34	0.273	$3.698 \cdot 10^3$	1.64
DUZDUX (Orthorhombic)					
hkl	Multiplicity	Area	% Area	Total area	% Total area
{0 0 2}	2	$1.51 \cdot 10^4$	21.140	$3.029 \cdot 10^4$	42.28
{0 -1 1}	4	$7.15 \cdot 10^3$	9.985	$2.861 \cdot 10^4$	39.94
{1 0 0}	2	$4.86 \cdot 10^3$	6.781	$9.714 \cdot 10^3$	13.56
{1 0 1}	4	755.40	1.055	$3.021 \cdot 10^3$	4.22

Table S4. Summarized properties of the predicted crystal morphologies. Apical faces area is calculated for one side only of the regular polyhedron.

	IFABEW	CCDC #1494530	DUZDUX
Aspect ratio	14.513	15.508	3.326
Volume (Å^3)	$4.225 \cdot 10^6$	$3.527 \cdot 10^6$	$1.233 \cdot 10^6$
Apical Faces area (Å^2)	$4.362 \cdot 10^3$	$3.698 \cdot 10^3$	$6.370 \cdot 10^3$

VI. Raman Scattering:

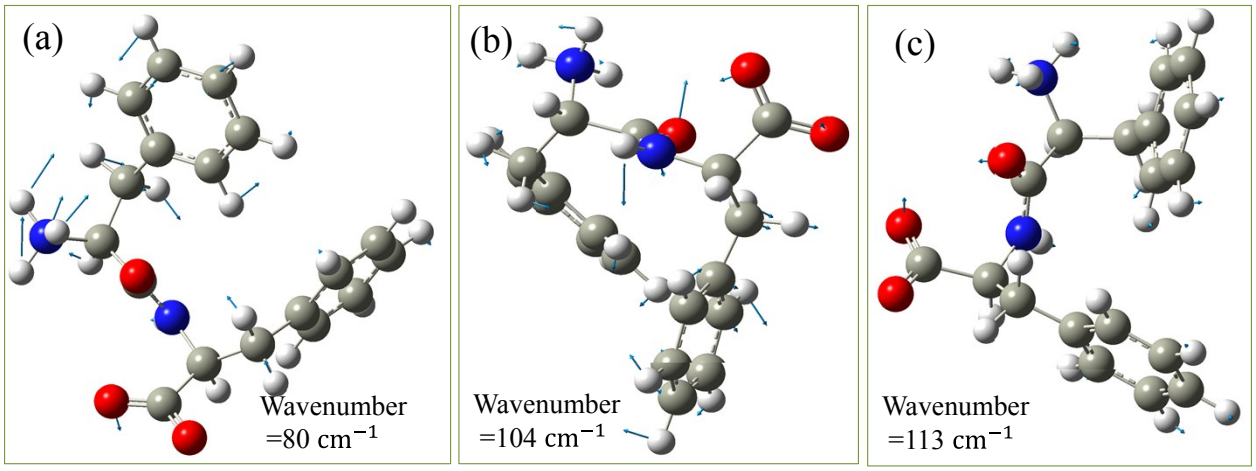

Figure S5. Displacement pattern of a FF molecule at (a) 80 cm^{-1}, (b) 104 cm^{-1}, and (c) 113 cm^{-1}.

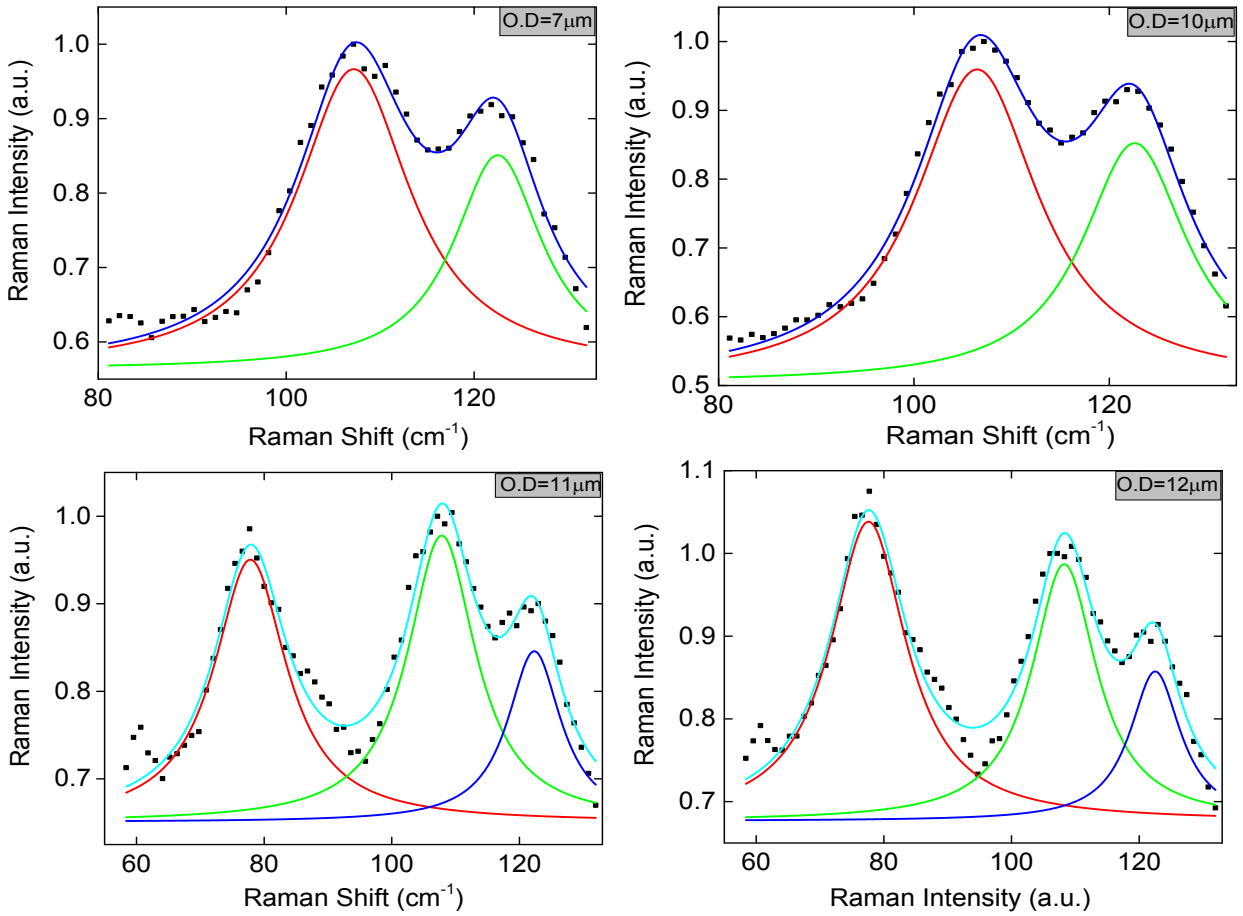

Figure S6: Peak fit of Raman scattering from individual FF-MNTs with varying O.D.s.

Table S5. Peak fit parameters from diameter dependent Raman data

Diameter (μm)	Peak Position	FWHM	Intensity ratio (80 cm^{-1}/107 cm^{-1})	Intensity ratio (107 cm^{-1}/122 cm^{-1})
7	No peak	---------	--------	1.4
	107	14		
	122	11.5		
10	No peak	---------	--------	1.3
	106.5	15.3		
	122.6	13		
11	77.8	13.8	0.9	1.7
	107.8	13		
	122.3	10.2		
12	77.6	14.5	1.2	1.7
	108.3	12.3		
	122.5	9.7		
13	77.1	16.5	1.8	2.2
	109.1	10.7		
	122.8	9.2		

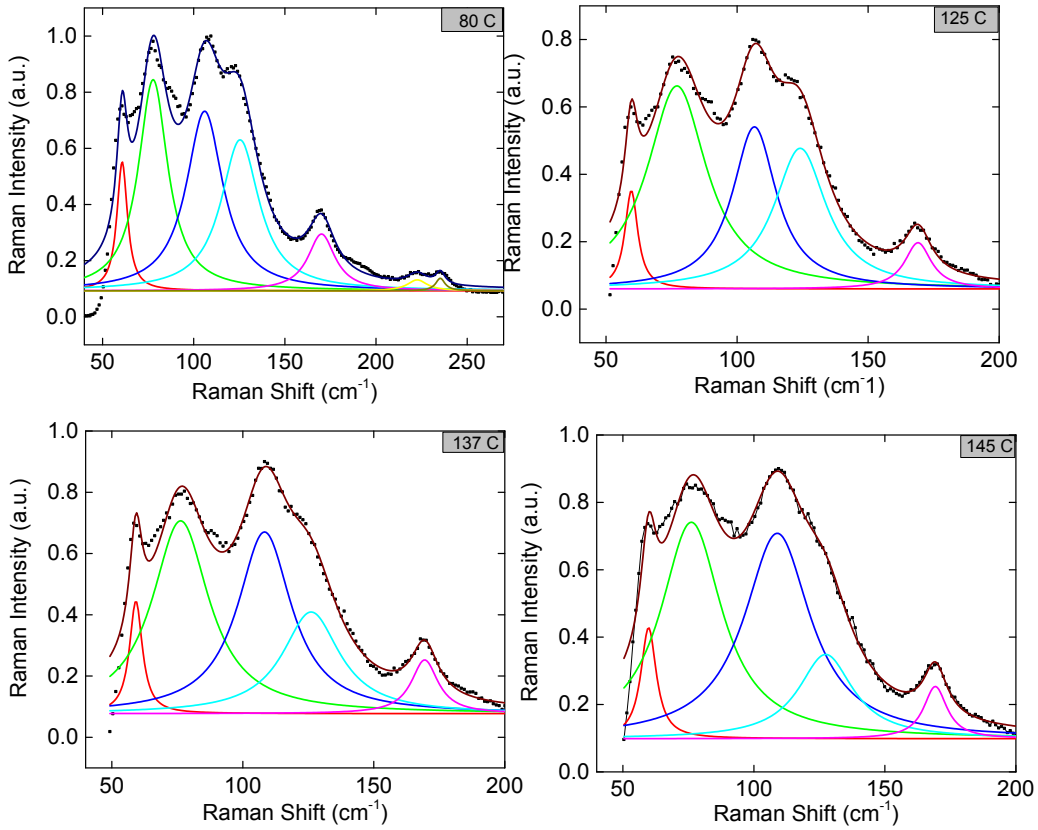

Figure S6: Peak fit of Raman spectra from FF-MNT (O.D. = 11 μm) at different annealing temperatures. Annealing the tube beyond 145 °C results in the orthorhombic phase.

Table S6. Peak fit parameters from temperature dependent Raman data

Temperature (C)	Peak Position (cm^{-1})	FWHM (cm^{-1})	Ratio of the intensity of two peaks
80	106.0±0.7	24.4±2.8	1.2
	125.4±0.9	25.5±2.3	
125	106.6±0.4	20.5±1.9	1.2
	124.0±0.7	24.3±1.6	
137	108.3±0.5	25.0±2.0	1.8
	126.0±1.1	26.0±2.5	
145	108.9±0.8	30.7±3.2	2.4
	127.0±1.5	25.2±3.9	